Corrosion Rate Study of AZ91C Magnesium Alloy in Sodium Chloride Solution of Different Concentrations Using Immersion Method for coated and Uncoated Samples[1]

Mohammed S. R. Saleh, Ali F. Ali Fadiel, Hafiez M.B.Khalida,

Higher Institute for Sciences and Technology, Tobruk, Libya

Received: 02 July 2023; Accepted: 24 August 2023; Published: 29 August 2023

ABSTRACT

For the investigation, the behavior of the die-cast magnesium alloy AZ 91C in air and a corrosive media containing various NaCl solution concentrations were examined. It was discovered that the life of magnesium alloy AZ91C is drastically reduced by the corrosive media (NaCl). The AZ91C alloy underwent chemical conversion treatment to increase its corrosion resistance. As demonstrated by immersion tests in various concentrations of NaCl al pH=7, the alloy's corrosion resistance was somewhat improved by conversion treatment in an alkaline stannite solution. MgSnO3.H2O can be seen in the X-ray diffraction pattern of the stannite-treated AZ91C alloy, and a porous structure that has been pierced by chloride ions can be seen in the SEM pictures. Increasing the NaCl content severely degrades the material's structure in the immersion test before coating. It subsequently reduces the material's resistance to corrosion. Despite the coating layer shielding the metal's surface during coating in a stannite alkaline solution, the NaCl progressively permeates into the structure of the Mg alloy. Finally, coated and uncoated samples were tested using theorem, an inhibitor, at various dosages to see what happened. Were determined using an immersion test.

Keywords: *Corrosion rate; Chemical conversion; corrosion resistance; immersion*

INTRODUCTION

Due to their extremely low density in comparison to other structural materials, high specific strength, excellent machinability and usability, and very low density, magnesium alloys are appealing for applications in the automotive, aerospace, communications, and computer industries. Magnesium is around 35% lighter than aluminum alloys and 65% lighter than titanium alloys due to its lower density of 1.738 g/cm3 at 20°C. Additionally, it has a strong damping capability and superior electrical conductivity. 24.32 is the atomic weight. [2] The hexagonal construction is compact. 650oC is the melting point while 1170oC is the boiling point. Thermal conductivity at 20 ºC is 157.5 W/mºC, and the specific heat is 1.030 kJ/kg ºC.

Magnesium alloys do have a low elastic modulus, a limited amount of toughness, and significant chemical activity (high affinity), which frequently results in low corrosion resistance. Numerous structural and nonstructural applications call for their utilization. Industrial, material handling, commercial, and aeronautical equipment are all examples of structural uses. Magnesium alloys are utilized in industrial machinery like textile and printing machines for parts that function at high speeds, therefore light weighing is necessary to reduce internal forces. Gravity conveyors, grain shovels, and dock decks are examples of material-handling machinery. The usage of luggage and ladders for business. [3] Good strength and stiffness at room and elevated temperatures coupled with light weight make magnesium alloys valuable for aerospace applications. Magnesium is a divalent metal with a silvery-white appearance. [4]

[1] *How to cite the article:* Saleh M.S.R., Fadiel A.F.A., Khalida H.M.B. (August, 2023); Corrosion Rate Study of AZ91C Magnesium Alloy in Sodium Chloride Solution of Different Concentrations Using Immersion Method for coated and Uncoated Samples, *International Journal of Advances in Engineering Research*, Vol 26, Issue 2, 7-17

EXPERIMENTAL WORK

Material

Cast alloy AZ91C was used as the test alloy. The tested material, AZ91C, whose chemical composition was used for all experiments in this study. The initial microstructure consists of two phases, α-phase and β-phase. The α phase is an Mg-Al-Zn solid solution with the same crystal structure as magnesium, and the β phase precipitate is an intermetallic phase - Mg17Al12, containing more than 40% aluminum. The free corrosion potential of this intermetallic compound segregated at grain boundaries is close to -1.0 V, while that of the α phase is -1.73 V [6]

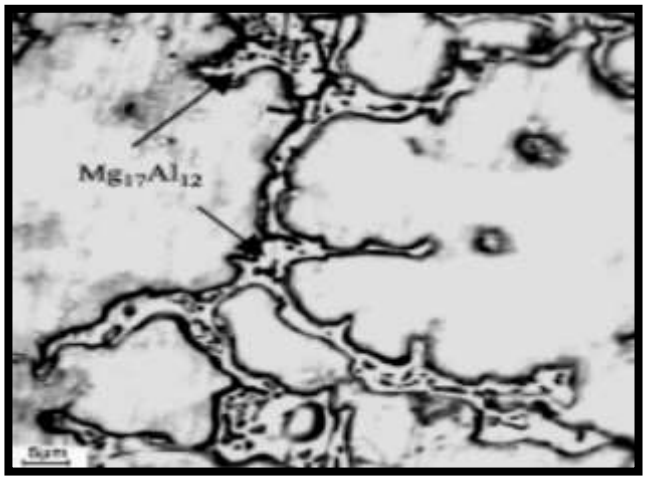

Fig. 1. Microstructure of AZ91C

Table I. Chemical Composition of AZ91C Mg alloy (wt. %) [7]

Alloy	*Mg*	*Al*	*Zn*	*Mn*	*Si*	*Cu*	*Fe*	*Be*
AZ91C	***BAL.***	***8.7***	***0.53***	***0.18***	***0.087***	***0.035***	***0.012***	***0.0004***

All test specimens were prepared by polishing with successive 280, 400, 800, and finally, 1200 grit papers, followed by cleaning, degreasing, and air drying.

Immersion tests in various conditions are used to gauge a material's corrosion resistance. For the immersion procedure, rectangular specimens with dimensions of 30 x 30 x 4.80 mm were utilized to calculate weight loss. Before and after the testing, the samples were cleaned, degreased, and weighed on an analytical scale (measuring precision 0.0001 g). Exams lasted for two days. Standard techniques were used to remove the corrosion products from the sample surfaces, which were then weighed following the test samples. In the accelerated corrosion experiments, additional specimens of identical size were employed. The mechanical characteristics of the alloy are shown in

Table II. Mechanical Properties of AZ91C Mg alloy [7]

Yield Strength, MPa	*Tensile Strength MPa*	*Elongation % in 50 mm gl.*	*Hardness HB*	*Elastic modulus GPa*
145	***275***	***6***	***68***	***45***

For durable immersion testing, samples were polished to 1200 grit on finer sandpaper, then polished with polishing pads and aluminum oxide. All samples were first cleaned according to the procedure of ASTM Standard G 172-03 [8]. Samples that had been polished and reweighed were exposed to solutions (1%, 3%, 5%, and 7% NaCl) for varying lengths of time. At the conclusion of the experiment, give the samples one last wash by submerging them in a solution of 15% CrO3 in 100 mL of boiling water. Then acetone was used to clean it. Following each trial, weight loss was recorded, and each mill's corrosion rate was determined [9]

Environment

Thiourea has been selected as the study's inhibitor. Full immersion tests were conducted in aqueous solutions of 1%, 3%, 5%, and 7% NaCl with a pH of 7. It was exposed for two days.

The presence of an inhibitor and 5% NaCl water solutions at pH = 7 were used for the full immersion testing. In 5% NaCl aqueous solutions, the total amount of inhibitory pigments was present at various concentrations (0.01, 0.03, 0.05, and 0.1 gm/l).

Weighing the examined samples after testing allowed us to calculate the corrosion rates. Corrosion products were eliminated for this reason.

Table III. Bath of stannite conversion coating

Composition	*Quantity*	*Operating condition*
Na2SnO3·3H2O	*50 gm/L*	*Temperature=60*
CH3COONa·3H2O	*6gm/L*	*^{o}C*
Na3PO4·12H2O	*50 gm/L*	*pH=12.3*
NaOH	*2 gm/L*	*Time=60 min*

The cross-sectional morphology of the chemical conversion coating is shown in Fig. 5. Spherical particles and conical gaps between them can be seen more clearly. After soaking for 60 minutes, the coating thickness reached 2 μm. In a tin ore bath at 60°C. [10]

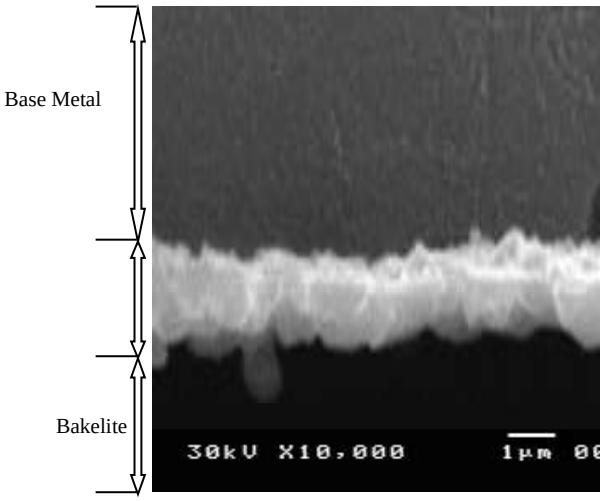

Fig. 2. Cross-section morphology for chemical conversion on Mg alloy AZ91C

Different Procedures of Experimental Work

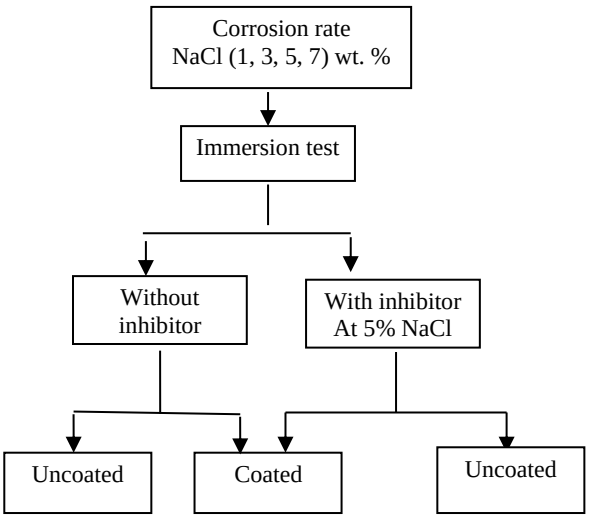

Fig. 3 is a flow chart showing experimental procedure tests that were used in this study.

RESULTS AND DISCUSSION

Several corrosion experiments were carried out in different NaCl concentrations to study and understand the corrosion behavior of AZ91C alloy the corrosion rate of the AZ91C sample as a function of the NaCl solution concentration was carried out during immersion for 48 hours.

Fig.7. shows the effect of NaCl concentration on corrosion rate before and after coating. It is clear that increasing NaCl concentration increases the corrosion rate in both cases (before and after coating). Before coating, it is found that the corrosion rate highly increases as the NaCl % increases. On the other hand, the corrosion rate of the coated samples gradually increased with the increase of NaCl content.

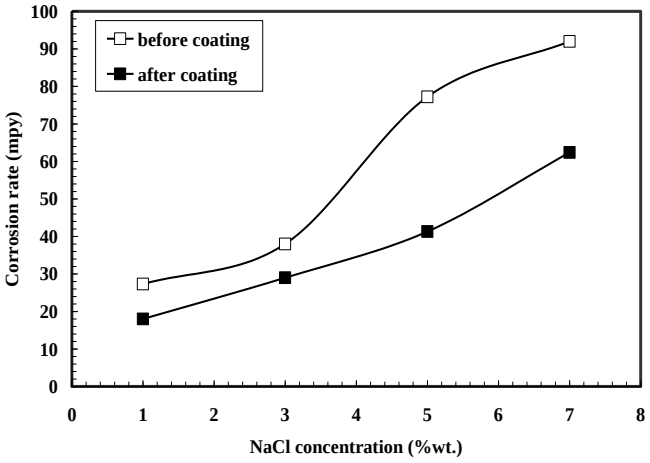

Fig.4. Effect of sodium chloride concentration on corrosion rate without inhibitor

However, the corrosion rate of the coated samples shows much lower corrosion pits than the uncoated ones. Fig.5. is an optical micrograph of AZ91C samples uncoated in 5%NaCl (with different concentrations of Thiourea). At 5-7% NaCl concentration, the corrosion rate of the Uncoated samples highly increase and this is emphasized by microstructure investigation shown in Fig.5.

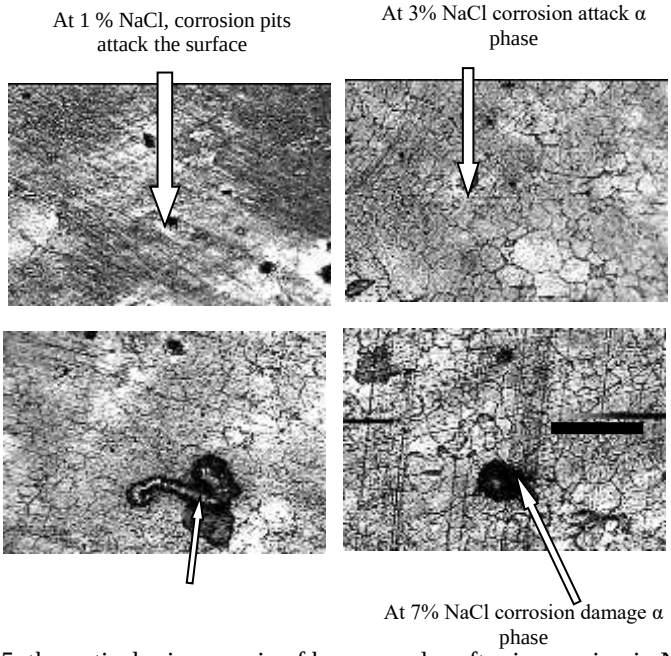

Fig.5. the optical microscopic of bare samples after immersion in NaCl solution at different concentrations, corrosion started initially al localized sites.

The surface corroded layer (corrosion pits) Uncoated AZ91C samples showed the presence of Mg (OH) 2 and NaClO4 as the main corrosive product as shown in the XRD spectra given in Figs. 6. And.7. which is formed as a result of the dissolution of Mg from the alloy surface in NaCl solution. The formation of corrosion pits results from the localized attack of chloride ions on the surface at the weak points in its surface film.

On the other hand, the coated samples of AZ91C show a much lower corrosion rate indicating the enhancement of the material corrosion resistance as a result of the coating effect see Fig.8. The microstructure after coating exhibits uniform light pits on the corroded surface due to coating protection. The products of that protected surface are clarified in XRD spectra as shown in Figs.9. & 10. Where (Mg Sn (OH) 6) sodium stannite appears. The corrosion protection of the coated samples is related to the presence of this layer (Mg Sn (OH) 6).

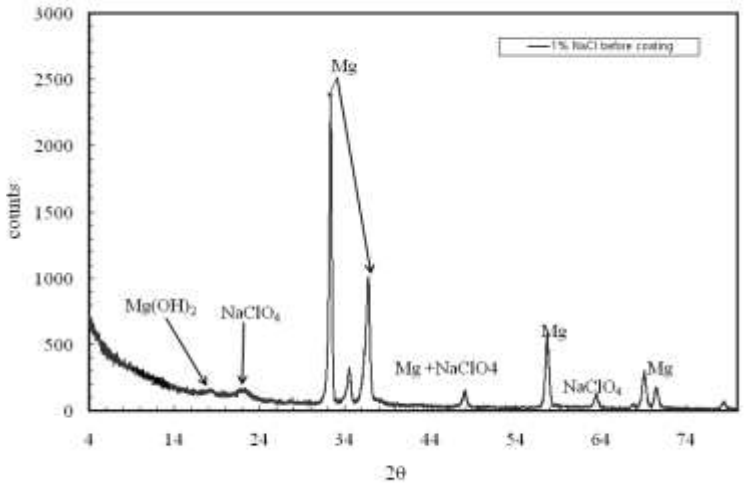

Fig.6. XRD Spectra of 1% NaCl without coating without inhibitor

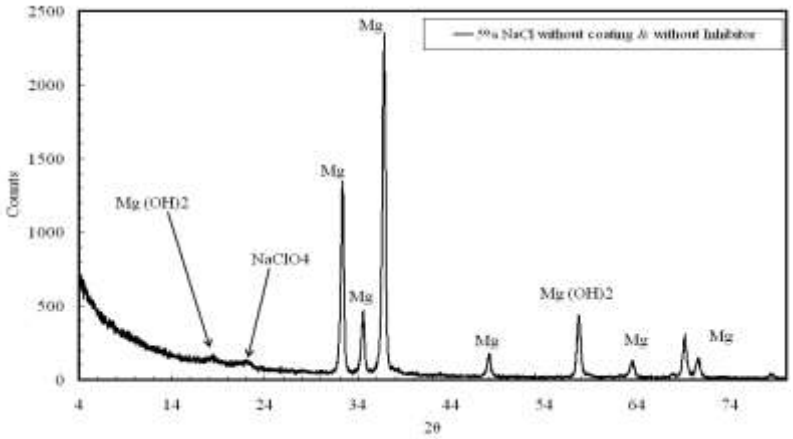

Fig.7. XRD Spectra of 5%NaCl without coating and without inhibitor

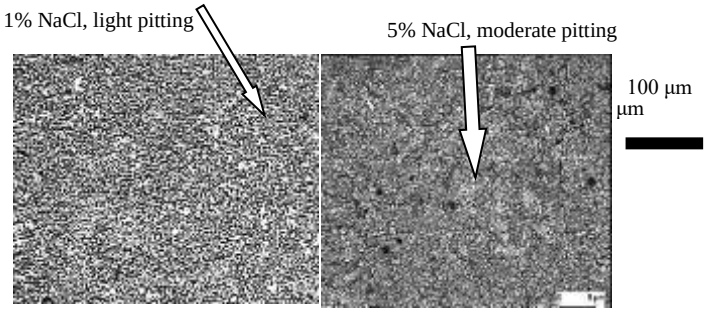

Fig.8. the optical photograph of coated samples

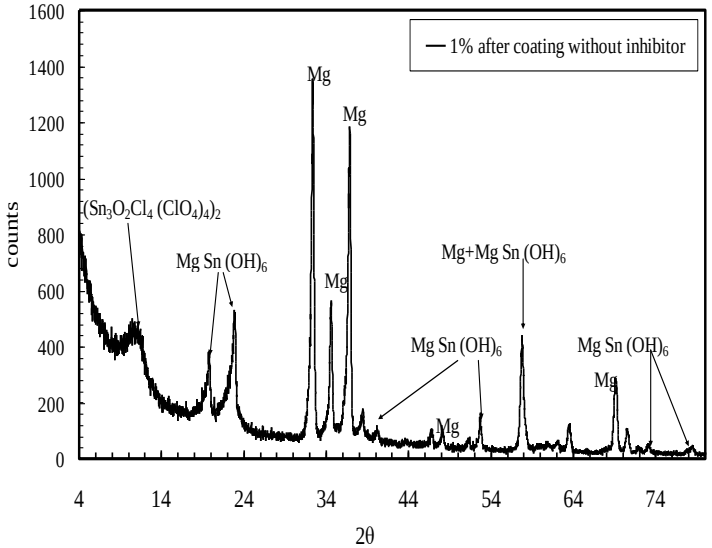

Fig.9. XRD Spectra of 1%NaCl after coating and without inhibitor

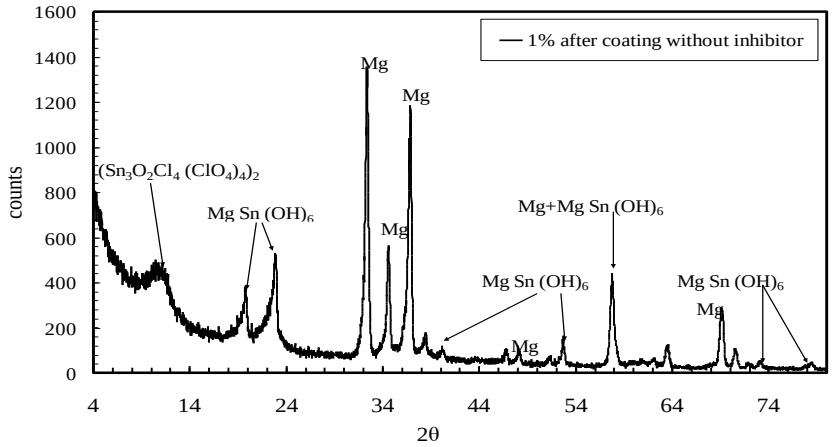

Fig.10. XRD Spectra of 1%NaCl after coating and without inhibitor

Figs. 5. And.8. Typical surface features of corroded surfaces after exposure are also shown. In both cases, corrosion initially starts locally, especially on the primary α phase. Localized corrosion penetrates the entire surface and sustains exposure, and results in a generalized corrosion mode in which multiple beta particles remain unaffected on the surface while the entire matrix is dissolved. The degree of attack and erosion of corrosive media.

Immersion tests in the presence of theorem inhibitor

The corrosion rates are determined after 48 h immersion of uncoated and coated samples in the presence of different concentrations of theorem as an inhibitor.

Fig. 11. Shows the effect of theorem concentration on corrosion rate of the coated and uncoated samples in 5% NaCl. The plots of figure indicate that the coated layer enhances the corrosion resistance as theorem percentage increases till a minimum certain value at 0.05g/l theorem (corrosion rate 17.67mpy), then corrosion rate increases again

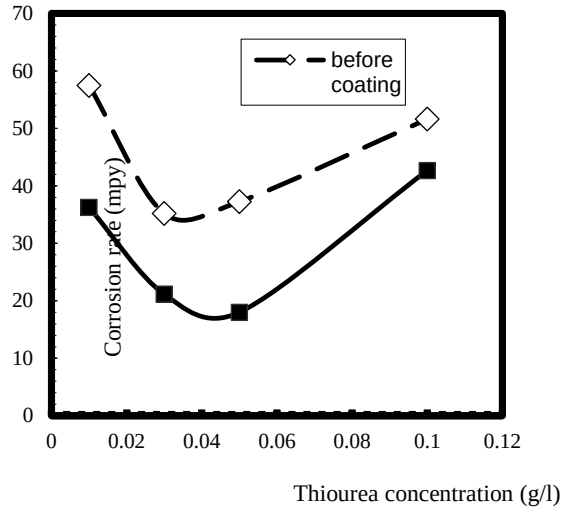

Fig.11. Effect of Theorem concentration on corrosion rate at 5%NaCl

Fig. 12. Shows an optical micrograph of AZ91C immersed in 5% NaCl before coating. It is found that the surface layer of AZ91C exhibits a high corrosion rate at 0.01 and 0.1g/l theorem due to the corrosion product. Figs.13. &.14. Are x-ray spectra of AZ91C after immersion in 5% NaCl. Fig.13. Shows NaClO4 and Mg (OH) 2 products. In addition, it is clear that the NaClO4 of Fig.13 is relatively higher than that of Fig.14. Consequently, the corrosion resistance enhanced at theorem concentrations 0.03 and 0.05 g/l theorem due to the minimum values of NaClO4 and Mg (OH) 2, see Figs. (13&14).

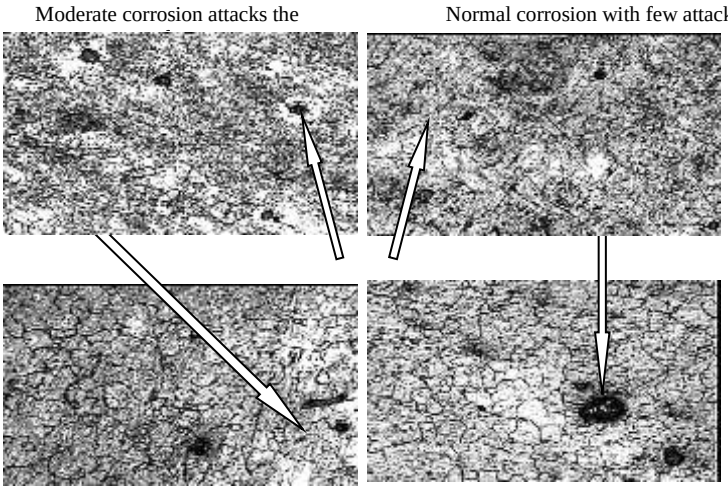

Fig.12. the optical samples after immersion in 5%

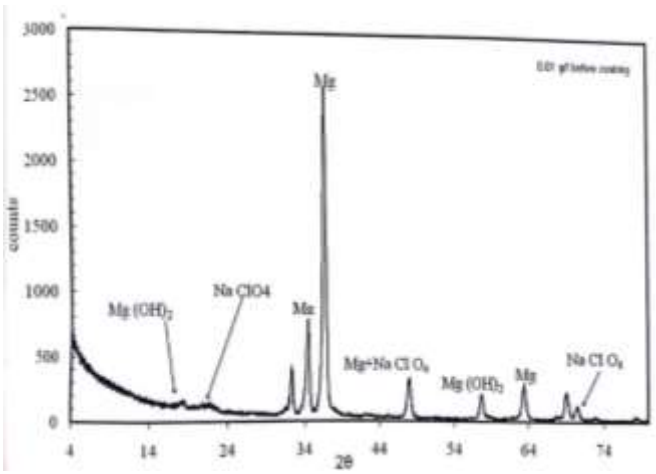

Fig.13 XRD Spectra after immersion in 5% NaCl before coating with 0.1 g/l Theorem

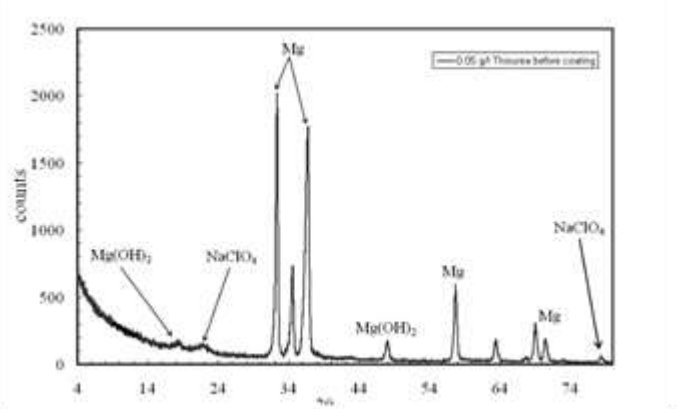

Fig.14 XRD Spectra after immersion in 5% NaCl before coating with 0.05 g/l Theorem

On the other hand, after coating, the corrosion resistance was highly enhanced due to the existence of stannite layer (Sn3O2Cl4 (ClO4)4)2 & Mg Sn (OH) 6, as shown in the optical microstructure in See Fig.15. Where corrosion pits are highly remarked at 0.01 and 0.1g/l theorem.

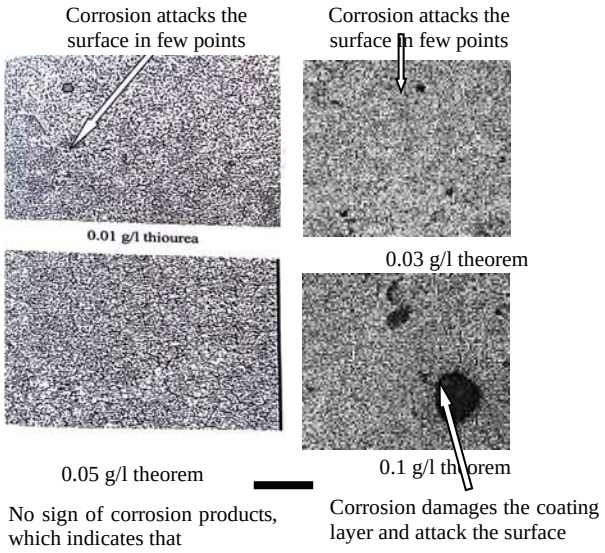

Fig.15. the optical microstructure of coated samples after immersion in 5% NaCl with different theorem concentrations after coating

The corrosion pits decrease at the theorem concentrations 0.03 and 0.05g/l. Figs.16. And .17.are x-ray spectra of AZ91C after coating and immersion in 5% NaCl in the presence of 0.05 and 0.1 g/l theorem respectively

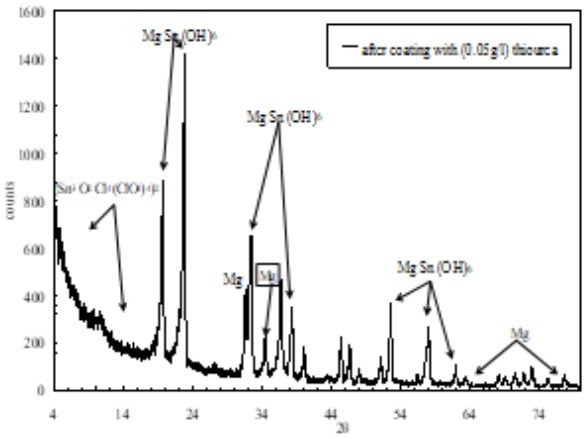

Fig. 16. XRD Spectra after immersion in 5% NaCl after coating with 0.05 g/l Thiourea

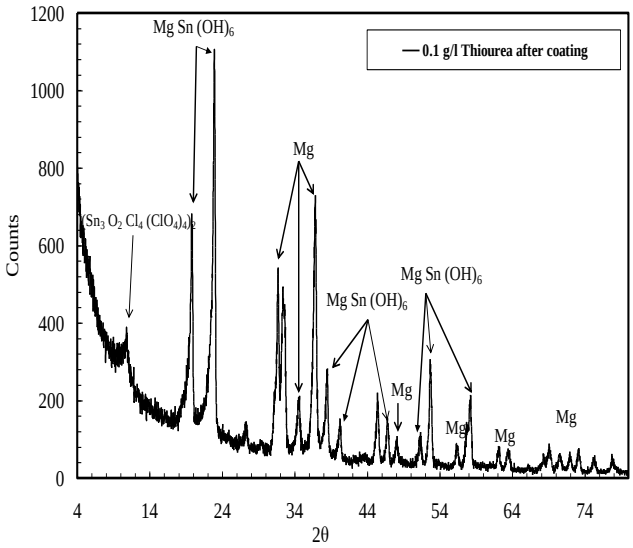

Fig. 17. XRD Spectra after immersion in 5% NaCl after coating with 0.1 g/l Thiourea

Inhibiting & coating efficiency of the immersion test (IE) is calculated by the equation:

$$IEorCE(\%) = \frac{C.R_{without} - C.R_{with}}{C.R_{without}} \times 100$$

Where:
C.R without: Corrosion rate without inhibitor or without a coat
C.R with: Corrosion rate with inhibitor or with coating

Table IV.

Percentage enhancing efficiency of the coating layer at various concentrations of NaCl (pH=7).

solution	***Inhibiting Efficiency (IE), %***
	Immersion test
5% NaCl + 0.01 g/l Thiourea	***25.5***
5% NaCl + 0.03 g/l Thiourea	***54.5***
5% NaCl + 0.05 g/l Thiourea	***51.8***
5% Na Cl + 0. 1 g/l Thiourea	***33.2***

Table V.

The percentage inhibition efficiency of Theorem in 5% NaCl (pH=7).

Solution	***coating Efficiency (CE), %***
	Corrosion rate (Immersion test)
1% NaCl	***34***
3% NaCl	***24***
5% NaCl	***46.5***
7% NaCl	***32.17***

Table VI.

Percentage enhancing the efficiency of both (coating & inhibitor) at 5% NaCl (pH=7)

solution	***Combined Efficiency (BE), %***
	Immersion test
5% NaCl + 0.01 g/l Thiourea	***53***
5% NaCl + 0.03 g/l Thiourea	***72.6***
5% NaCl + 0.05 g/l Thiourea	***76.7***
5% NaCl + 0. 1 g/l Thiourea	***44.4***

CONCLUSIONS

1. Corrosion pits are formed at the boundaries of β-grains in the α-Mg matrix
2. Water immersion test; the results show that the conversion coating in a stannous alkaline bath improves the corrosion resistance of AZ91C-Mg alloy.
3. The conversion coating thickness is approximately 2 µm with lots of non-penetrating pores.
4. The stannite coating bath is capable of producing uniform coating.
5. The coating layer improves the corrosion rate from 77.2 mpy to 41.3 mpy at 5% NaCl (46.5%).
6. The thiourea inhibitor improves the corrosion rate of uncoating Mg alloy AZ91C from 77.2 mpy to 35.2 mpy at 0.03 g/l TU (54.5%) and coated Mg-alloy AZ91C from 41.3 mpy to 18 mpy at 0.05 g/l TU (56.4%).
7. For uncoating samples, fatigue emanated crack initiates at the surface, while it is at corrosion pits.
8. For coated sample NaCl solution leads to a defect in the coating layer
9. Conversion coating in stannite bath improves the fatigue life from 55300 cycles to 107000 cycles at 7% NaCl (93.5%).

REFERENCES

1. Feliu Jr, S., Pardo, A., Merino, M. C., Coy, A. E., Viejo, F., & Arrabal, R. (2009). Correlation between the surface chemistry and the atmospheric corrosion of AZ31, AZ80, and AZ91D magnesium alloys. Applied Surface Science, 255(7), 4102-4108.
2. Yan, C., Ye, L., & Mai, Y. W. (2004). Effect of constraint on tensile behavior of an AZ91 magnesium alloy. Materials Letters, 58(25), 3219-3221.
3. Avedesian M. M. Baker H. & ASM International Handbook Committee. (1999). Magnesium and magnesium alloys. ASM International.
4. Hapeta, P., Kerkhoven, E. J., & Lazar, Z. (2020). Nitrogen is the major factor influencing gene expression in Yarrowia lipolytica. Biotechnology Reports, 27, e00521.
5. Gao, W., & Liu, Z. (2009). U.S. Patent Application No. 12/158,535.
6. Y. Sokata, ASEF SURIFIN 87, conf. Mexico, (2005). Proc P-6.
7. Potziesc, kainer U K. "Fatigue of magnesium alloys". Advanced Engineering Material, (2004), 6(5): pp. 281-289.
8. Zhou W. Aung N. N. & Sun Y. (n.d.). Effect of antimony bismuth and calcium addition on corrosion and electrochemical behavior of az91 magnesium alloy. Corrosion Science 403–408. https://doi.org/10.1016/j.corsci.2008.11.006
9. Ambat R. Aung N. N. & Zhou W. (n.d.). Evaluation of microstructural effects on corrosion behavior of az91d magnesium alloy. Corrosion Science 1433–1455. https://doi.org/10.1016/S0010-938X(99)00143-2
10. Huo, H., Li, Y., & Wang, F. (2004). Corrosion of AZ91D magnesium alloy with a chemical conversion coating and electroless nickel layer. Corrosion Science, 46(6), 1467-1477.